

Combustion Product Formation in Under and Overventilated Full-Scale Enclosure Fires

WILLIAM M. PITTS, NELSON P. BRYNER, and ERIK L. JOHNSON

Building and Fire Research Laboratory
National Institute of Standards and Technology
Gaithersburg, MD 20899

INTRODUCTION

The findings of an extensive series of over 140 natural gas fires in a 2/5ths-scale model of a standard room have been previously reported [1]. The current work extends the earlier reduced-scale enclosure (RSE) study to a full-scale enclosure (FSE) and focuses on comparing the gas concentrations and temperatures of the upper layers. Both studies are part of a larger research effort [2,3] which is designed to provide a better understanding and predictive capability for the generation of carbon monoxide, the major toxicant in fires [4,5,6,7]. The findings will be incorporated into realistic fire models and used in the development of strategies for reducing the number of deaths attributed to carbon monoxide.

EXPERIMENTAL

The FSE is based on a standard fire-test room prescribed by ISO [8] and ASTM [9] which is 2.44 m wide \times 2.44 m high \times 3.67 m deep with a 0.76 m wide \times 2.03 m high door centered at the bottom of the front wall. The room consisted of a sheet metal stud framework which was lined with three layers of 1.27-cm-thick gypsum wallboard and a single layer of 1.27-cm-thick calcium-silicate board. Two vertical trees of 33 bare chromel-alumel thermocouples were utilized to monitor temperatures within the enclosure, and a third tree of ten aspirated thermocouples was used to track temperatures across the doorway. The inside trees were placed 50 cm from a side wall and 50 cm from the front and rear walls. Two additional platinum-rhodium thermocouples were incorporated after some of the temperatures generated during the fires were discovered to have exceeded the upper range (1260°C) for chromel-alumel thermocouples. Cooled and uncooled extraction probes were positioned at different locations to allow individual CO, CO₂, and O₂ gas analyzers to sample the upper combustion layer, lower layer, and outside the doorway. Temperature data from the aspirated thermocouples were used in tandem with inside thermocouple measurements to calculate doorway mass flows using a recently developed algorithm [10,11]. The 35-cm-diameter burner, which was scaled to maintain the same fuel exit velocities as in the RSE, was centered in the enclosure with the burner lip 38 cm above the floor. Fire size was controlled by setting the metered flow of the natural gas fuel.

The reduced-scale enclosure was designed to be a 40%-scale model of the standard room and has been previously described [1]. Briefly, the overall dimensions of the RSE were scaled geometrically from those for the FSE resulting in a RSE with internal dimensions of 0.98 m wide \times 0.98 m high \times 1.46 m deep. The area for the RSE doorway was determined using the $Ah^{1/2}$ enclosure ventilation scaling parameter, where A is the geometrically scaled total area of the ventilation opening and h is the height of the opening [1,12]. This resulted in a 0.48 m wide \times 0.81 m high door for the RSE. The RSE steel frame was first lined with sheet metal to form an airtight enclosure before two layers of 1.27-cm-thick calcium-silicate board were added to become the inner walls. As in the FSE, two thermocouple trees were utilized to monitor temperatures within the enclosure, and a tree of five aspirated thermocouples was used to track temperatures across the doorway. A tree of seven chromel-alumel thermocouples was located in a rear corner, 20 cm from the side wall and 20 cm from the rear wall. A tree of 17 thermocouples was positioned in a front corner 20 cm from the side wall and 20 cm from the front wall. Cooled and uncooled probes were positioned at different locations to allow individual CO, CO₂, and O₂ gas analyzers to sample the upper combustion layer, lower layer, and outside the doorway. The doorway mass flows were calculated using the same algorithm as for the FSE. The 15-cm diameter burner was centered in the enclosure with the burner lip 15 cm above the floor.

Both the FSE and RSE were located under large instrumented exhaust hoods which allowed gas analysis and oxygen calorimetry [13,14] to be performed on the exhaust gases from the enclosures.

Each fire conducted in the RSE or FSE typically lasted 15 to 20 minutes. While over 140 fires with heat-release rates (HRRs) ranging from 7 to 650 kW were burned within the RSE, a more limited series of twelve fires ranging from 450 kW to 3500 kW were completed within the FSE. Fires of greater than 200 kW and 1250 kW HRR created underventilated conditions within the RSE and FSE, respectively.

RESULTS AND DISCUSSION

The data from the RSE and FSE allow comparisons of the upper-layer gas concentrations and temperatures for overventilated, near-stoichiometric, and underventilated conditions. Pairs of fires, one from the RSE and one from the FSE, having roughly the same global equivalence ratio (GER), defined as the mass in the upper layer derived from the fuel divided by the mass derived from the air normalized by the mass ratio for stoichiometric burning, are considered. The front and rear upper-layer CO and O₂ gas concentrations for both enclosures are plotted as a function of time for overventilated fires (Figures 1 and 2), near-stoichiometric fires (Figures 3 and 4), and underventilated fires (Figures 5 and 6). Front and rear upper-layer temperatures are also plotted for each fire size (Figures 7-9). The GER values for the different fires are listed in Table 1.

Scaling the RSE doorway via the Ah^{1/2} ventilation parameter proved to be quite good. The Ah^{1/2} scaling incorporates the square of a geometric scaling factor which was 0.4 for the RSE. On going from the RSE to the FSE, an increase by a factor of 6.25 (i.e. (1/0.4)²) is expected for the mass flow rate into the FSE for a given GER. As Table 1 indicates, the increases in mass flow rates from the RSE to the FSE are consistently a factor of 6.6 or 6.7. These are equal to the predictions within experimental uncertainty. After completing over 140 of the RSE burns, and before actually igniting any of the fires in the FSE, several scaling techniques were used to estimate the heat release rate sufficient to just underventilate the FSE. The Ah^{1/2} ventilation parameter calculation predicted that the FSE would become underventilated at 1250 kW. The observed value where the oxygen concentrations approached zero in both the front and rear of the upper layer of the RSE was 1400 kW.

For overventilated conditions in both enclosures, the measured concentrations of CO (Figure 1) were uniformly low, less than 0.25%. The oxygen concentrations (Figure 2) in the upper layer of the RSE dropped to about 7% in both the front and rear, but the upper layer of the FSE was not as uniform with front and rear concentrations of O₂ dropping to 9% and 5%, respectively. As the fuel flow rates were increased, the RSE and the FSE became less overventilated, and the oxygen concentrations in the upper layers decreased until they reached near zero for heat release rates of around 200 kW and 1400 kW, respectively. For both near-stoichiometric fires shown in Figures 3 and 4, the upper-layer O₂ concentrations approached zero in the rear of the enclosures while in the front of the enclosure the oxygen concentrations were not completely

Table 1. Fuel and Air Mass Flows Into the RSE and FSE

Heat Release Rate, kW	Fuel Mass Flow Rate to Burner (g/s)	Air Mass Flow Rate into Door (g/s)	Total Mass Flow Rate into Enclosure (g/s)	Global Equivalence Ratio	Ratio of FSE Flow to RSE Flow
100 (RSE)	1.7	59.1	60.8	0.6	6.7
850 (FSE)	16.2	389	405	0.7	
200 (RSE)	3.4	58.7	62.1	1.0	6.7
1250 (FSE)	23.2	395	418	1.0	
400 (RSE)	7.6	56.1	63.7	2.3	6.6
2700 (FSE)	50.3	342	392	2.4	
Notes: Each mass flow rate was averaged over a 660 second time period. Mass flow rate algorithm uses an iterative approach which forces the air and fuel mass flow rates into and the mass flow rate out of the enclosure to be equal [11].					

depleted with 2% and 3% measured in the RSE and FSE, respectively. The CO concentrations for the front and rear of the RSE upper layer averaged about 1%, but with a large amount of scatter in the data. In the rear of the FSE upper layer, the carbon monoxide concentrations slowly approached the values observed in the RSE. The concentrations of CO in the front of the FSE upper layer were 0.2%, significantly lower than the rear.

For the most underventilated conditions, the upper layers of both the RSE and FSE were completely depleted of oxygen. The upper layers of both compartments had higher concentrations of carbon monoxide as compared to the overventilated and near-stoichiometric cases. The distribution of CO within the upper layer was very different for the two enclosures with higher concentrations observed in the rear of the FSE and in the front of the RSE. The RSE upper-layer concentrations were 2.2% and 1.8%, front and rear, while the corresponding concentrations for the FSE ranged from 2.2 - 4.6% and 3.4 - 5.2%, front and rear, respectively. The concentrations of CO in the FSE upper layer were still increasing when the fire was terminated.

Ideally one would hope the quantitative concentration behaviors of combustion gases would be similar in the RSE and FSE. However, it is clear that the concentrations of carbon monoxide and oxygen are not as well behaved as the mass flow rates. The good agreement with predicted mass flows and the corresponding lack of agreement for combustion gas concentrations indicate that the generation of combustion products is not entirely controlled by the ventilation behaviors of the enclosures.

Temperature profiles for both the RSE and FSE from chromel-alumel thermocouples located in the upper layers are plotted in Figures 7 (overventilated), 8 (near-stoichiometric) and 9 (underventilated). These temperatures were recorded 80 cm and 200 cm above the floor, for the RSE and FSE, respectively. The plots indicate that the FSE upper-layer temperatures were typically 100° to 200°C hotter than the reduced-scale compartment. These higher temperatures are probably a result of the relatively wider doorway and reduced wall-surface area in the RSE. The area of the doorway of the RSE is a larger fraction of the front wall than in the FSE, and a higher fraction of the heat released within the enclosure is likely to be lost via radiation through the opening. The RSE also has a relatively greater wall surface area to total volume ratio than the FSE, so a greater fraction of heat can be lost by conduction through the walls of the RSE. The temperature profiles for both enclosures demonstrate that temperatures in the front of the enclosures were hotter than in the rear. The largest differences were for the RSE where temperature differences of up to 300°C were observed.

Since temperatures in the upper layer of the FSE exceeded the upper range of chromel-alumel thermocouples, a pair of platinum-rhodium thermocouples were installed for 2300 and 3500 kW fires (not shown). In the 3500 kW fire, front and rear temperatures peaked at 1200° and 950°C, respectively. Slightly higher temperatures were observed in the front and rear, 1300° and 1000°C, respectively, for the 2300 kW fire. These higher temperatures provide a possible explanation for the much higher concentrations of CO observed in the FSE as compared to the RSE. Pitts [15] has used detailed kinetic modeling to show that mixtures of rich combustion gases begin to come into thermodynamic equilibrium for temperatures on the order of 1100°C. At these temperatures the formation of CO is strongly favored over CO₂, and production of CO is therefore expected. The fact that the CO concentrations (Figure 5) and temperature (Figure 9) seem to increase together supports this conclusion. Temperatures in the RSE are too low for the reactions responsible for bringing the combustion gases into thermodynamic equilibrium to be important.

CONCLUSIONS

The reduced-scale and full-scale enclosure burn series allow a comparison of the compositions and temperatures of the upper layers and the ventilation behaviors for two geometrically similar compartments. The Ah^{1/2} ventilation scaling technique does an excellent job of scaling the mass flows into and out of the two enclosures. The ventilation-scaling technique (i.e., the GER) did not successfully predict the composition or temperature of combustion products in the upper layers when attempting to scale-up from the smaller to the larger compartment. The FSE burns generated significantly higher upper-layer carbon monoxide concentrations than observed in the RSE burns. Carbon monoxide concentrations of about 6% were measured in the front and rear of the FSE during higher HRR fires. These CO levels are two times higher

than the concentrations observed in the reduced-scale enclosure burns and about three times higher than those reported by previous researchers conducting idealized hood experiments [16,17,18]. Temperatures in the upper layer of the FSE are significantly higher than in the RSE providing an explanation for the higher CO concentrations observed as compared to the RSE. The front regions of the upper layers in both enclosures have significantly higher temperatures than the rear. The results of this investigation show that great care must be utilized when attempting to utilize experimental findings to predict temperatures or combustion-gas concentrations in full-scale fire tests.

REFERENCES

1. Bryner, N. P., Johnsson, E. L., and Pitts, W. M., *Carbon Monoxide Production in Compartment Fires - Reduced-Scale Enclosure Test Facility*, National Institute of Standards and Technology Internal Report, NISTIR 5568, December, 1994.
2. Pitts, W. M., *Executive Summary for the Workshop on Developing a Predictive Capability for CO Formation in Fires*, National Institute of Standards and Technology Internal Report, NISTIR 89-4093, April, 1989.
3. Pitts, W. M., *Long-Range Plan for a Research Project on Carbon Monoxide Production and Prediction*, National Institute of Standards and Technology Internal Report, NISTIR 89-4185, May, 1989.
4. Harland, W. A., and Anderson, R. A., *Proceedings Smoke and Toxic Gases from Burning Plastics*, January 6-7, 1982, London, England, p. 15/1.
5. Hill, I. R., *Am. J. Forensic Med. Path.* 10:49-53 (1989).
6. Harwood, B., and Hall, J. R., *Fire J.* 83:29-34 (1989).
7. Birky, M. M., Halpin, B. M., Caplan, Y. H., Fisher, R. S., McAllister, J. M., and Dixon, A. M. *Fire Mater.* 3:211-217 (1979).
8. *Fire Tests - Full-Scale Test for Surface Products*, Draft International Standard ISO/DIS 9705, International Organization for Standardization, Geneva, Switzerland, 1991.
9. *Proposed Method for Room Fire Test of Wall and Ceiling Materials and Assemblies*, American Society for Testing and Materials, Philadelphia, PA, 1982.
10. Janssens, M., and Tran, H., *J. Fire Sciences* 10:528-555 (1992).
11. Johnsson, E. L., Bryner, N. P., and Pitts, W. M., "Fire-Induced Mass Flow into a Reduced-Scale Enclosure," *Fire Safety J.*, submitted for publication (1995).
12. Quintiere, J. G., *Fire Safety J.* 15:3-29 (1989).
13. Twilley, W. H., and Babrauskas, V., *User's Guide for the Cone Calorimeter*, National Bureau of Standards Special Publication 745, 1988.
14. Huggett, C., *Fire Materials* 4:61-65 (1980).
15. Pitts, W. M., "Application of Thermodynamic and Detailed Chemical Kinetic Modeling to Understanding Combustion Product Generation in Enclosure Fires," *Fire Safety J.* (1995) to appear.
16. Beyler, C. L., *Fire Safety J.* 10:47-56 (1986).
17. Zukoski, E. E., Toner, S. J., Morehart, J. H., and Kubota, T., *Fire Safety Science--Proceedings of the First International Symposium*, Grant, C. E., and Pagni, P. J., eds., Hemisphere, New York, 1988, p. 295.
18. Zukoski, E. E., Morehart, J. H., Kubota, T., and Toner, S. J., *Combust. Flame* 83: 325-332 (1991).

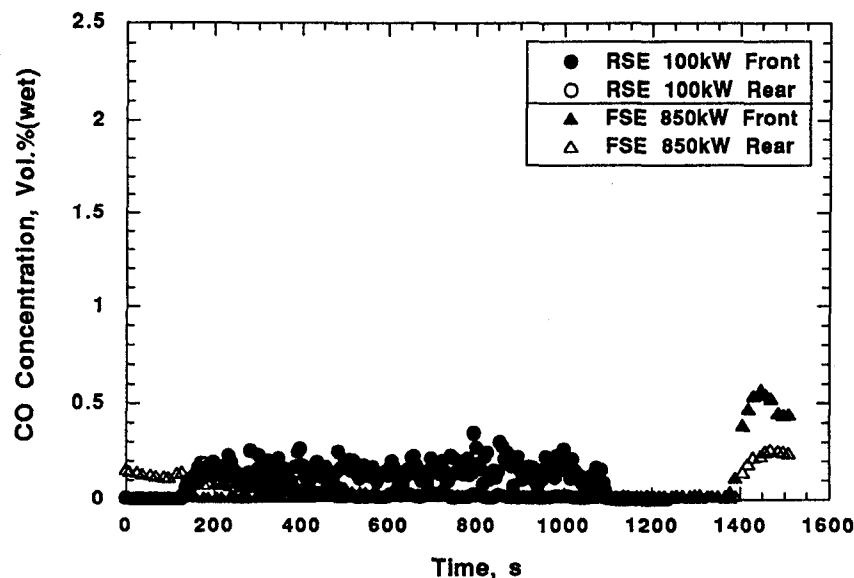


Figure 1. Upper layer carbon monoxide concentrations in the RSE and FSE versus time for two overventilated fires.

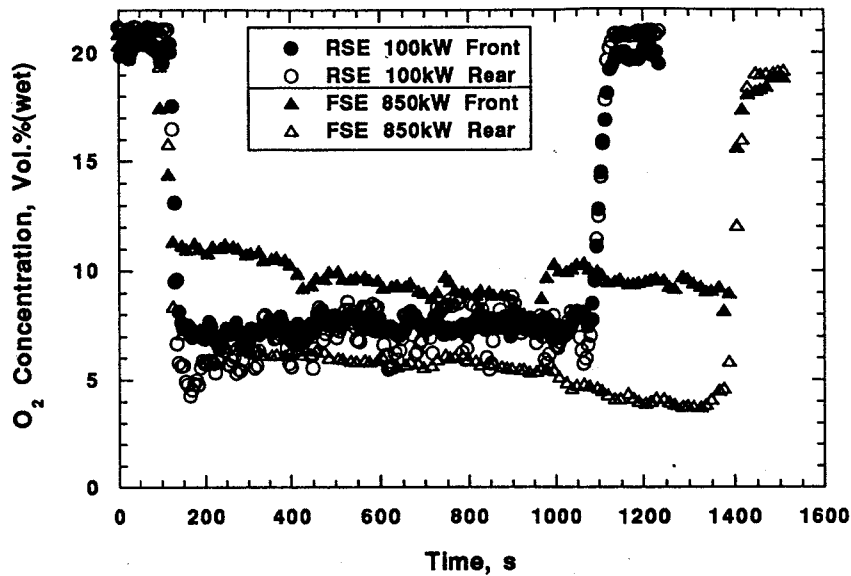


Figure 2. Upper layer oxygen concentrations in the RSE and FSE versus time for two overventilated fires.

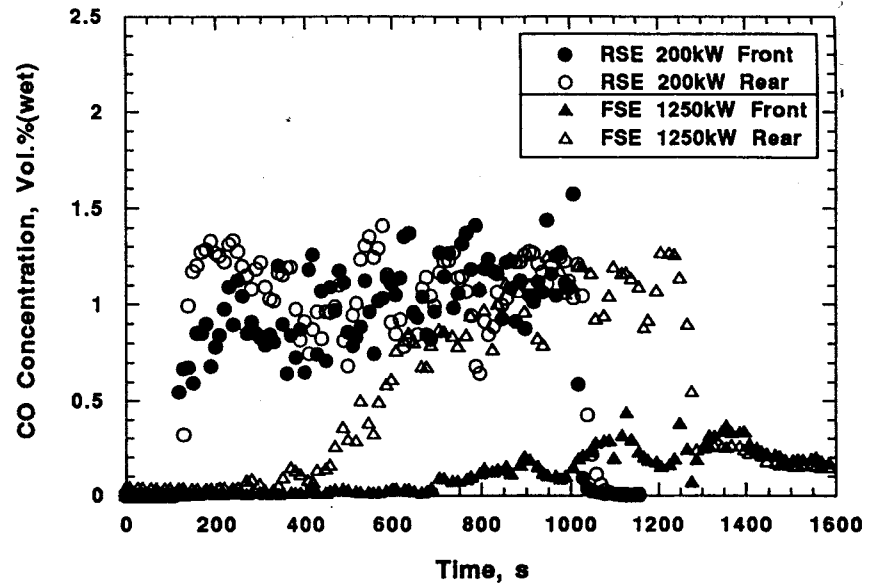


Figure 3. Upper layer carbon monoxide concentrations in the RSE and FSE for two near-stoichiometric fires.

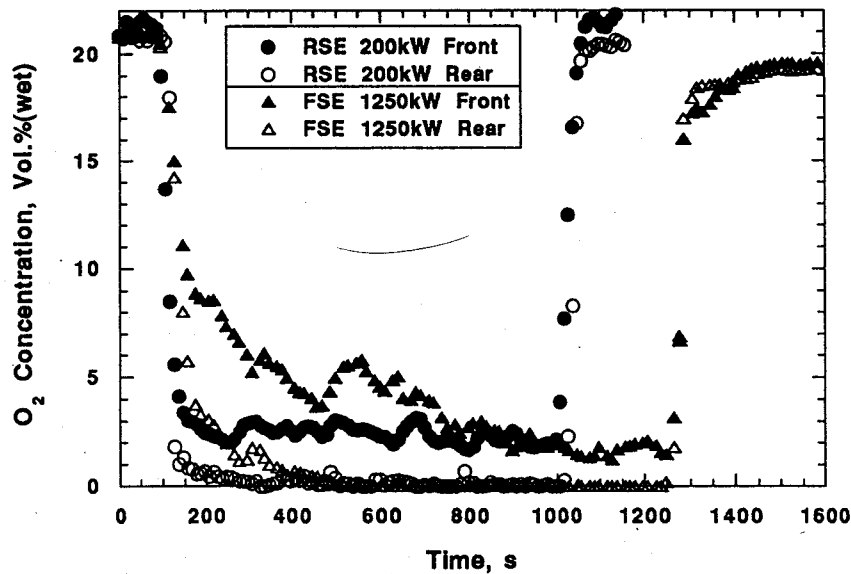


Figure 4. Upper layer oxygen concentrations in the RSE and FSE versus time for two near-stoichiometric fires.

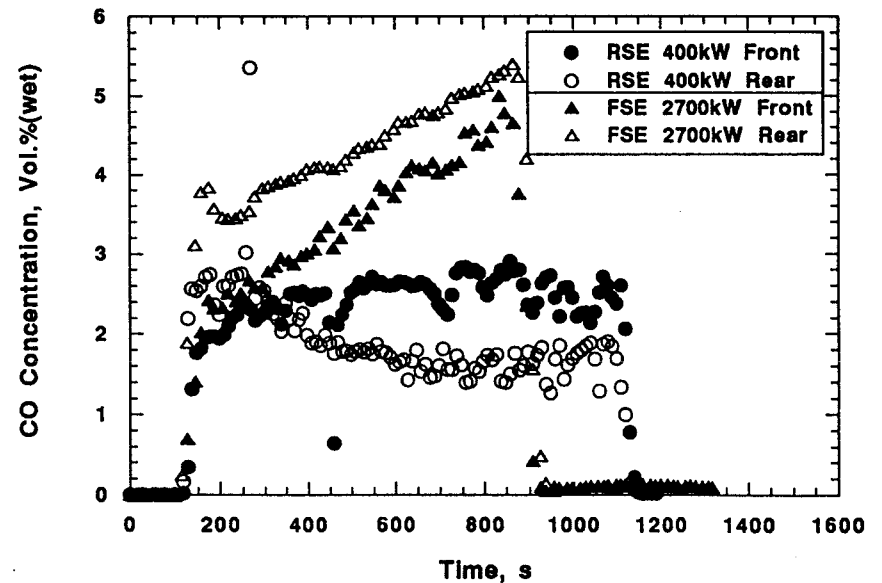


Figure 5. Upper layer carbon monoxide concentrations in the RSE and FSE versus time for two underventilated fires.

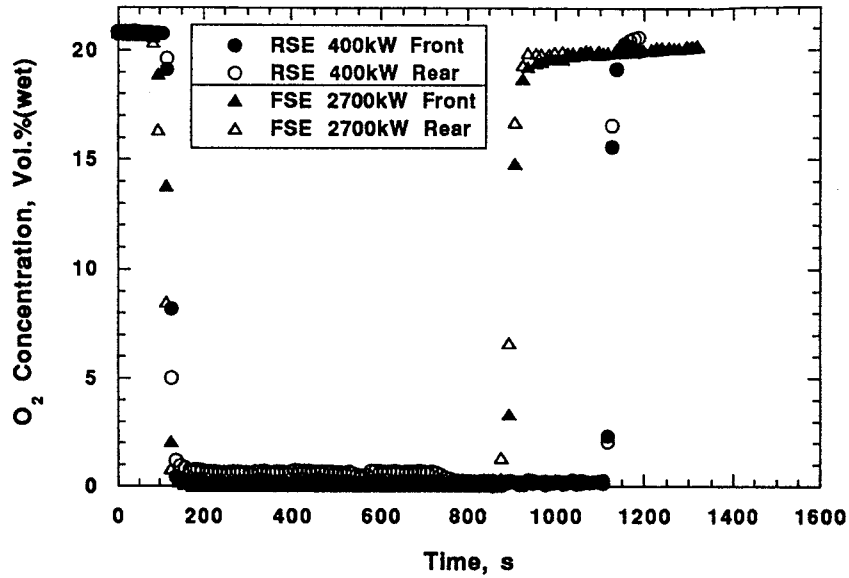


Figure 6. Upper layer oxygen concentrations in the RSE and FSE versus time for two underventilated fires.

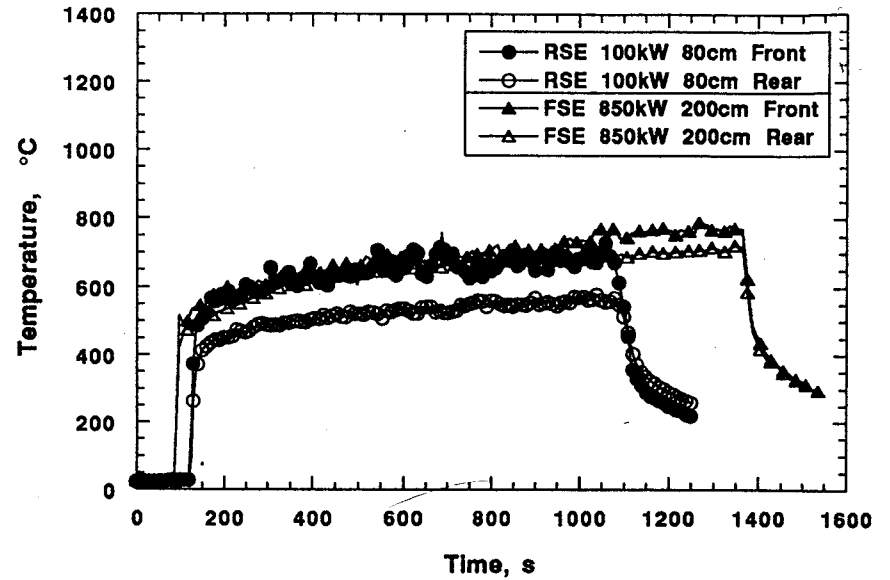


Figure 7. Temperatures in the RSE and FSE versus time for two overventilated fires.

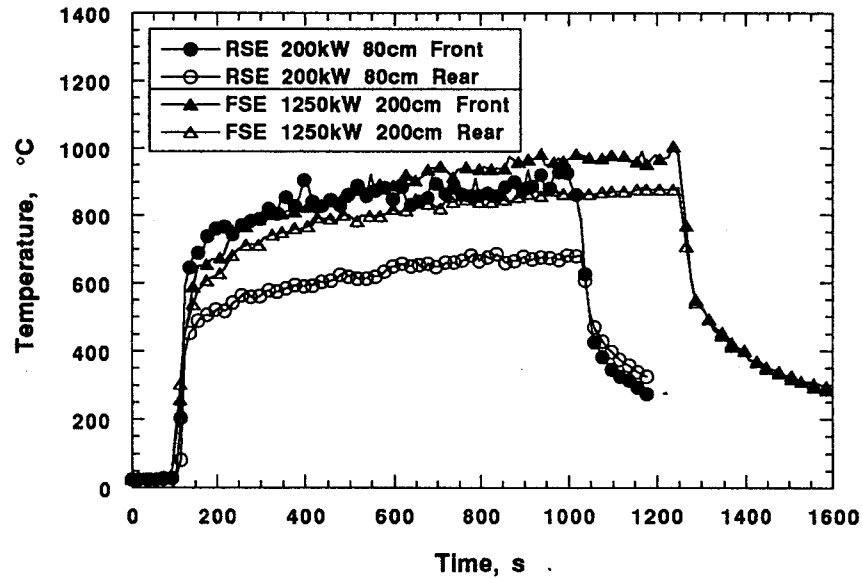


Figure 8. Temperatures in the RSE and FSE versus time for two near-stoichiometric fires.

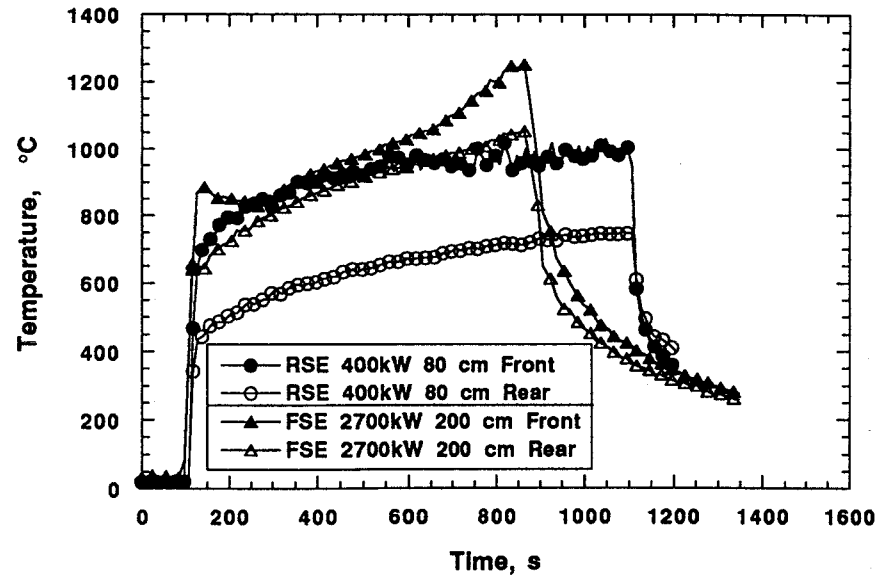


Figure 9. Temperatures in the RSE and FSE versus time for two underventilated fires.